

Theoretical study of (e, 2e) triple differential cross section of $1b_{3g}$ orbital of ethylene by vibrational multi-center distorted-wave method

Zhenpeng Wang(王振鹏), Maomao Gong(宫毛毛), Xingyu Li(李星宇), Songbin Zhang(张松斌), and Xiangjun Chen(陈向军)

Citation: Chin. Phys. B, 2023, 32 (**11**): 110205. DOI: 10.1088/1674-1056/acec45
Journal homepage: http://cpb.iphy.ac.cn; http://iopscience.iop.org/cpb

What follows is a list of articles you may be interested in

Structure of continuous matrix product operator for transverse field Ising model: An analytic and numerical study

Yueshui Zhang(张越水) and Lei Wang(王磊)
Chin. Phys. B, 2022, 31 (**11**): 110205. DOI: 10.1088/1674-1056/ac8a8f

Theoretical study of (e, 2e) triple differential cross sections of pyrimidine and tetrahydrofurfuryl alcohol molecules using multi-center distorted-wave method

Yiao Wang(王亦傲), Zhenpeng Wang(王振鹏), Maomao Gong(宫毛毛), Chunkai Xu(徐春凯), and Xiangjun Chen(陈向军)
Chin. Phys. B, 2022, 31 (**1**): 010202. DOI: 10.1088/1674-1056/ac21c3

Real-space parallel density matrix renormalization group with adaptive boundaries

Fu-Zhou Chen(陈富州), Chen Cheng(程晨), and Hong-Gang Luo(罗洪刚)
Chin. Phys. B, 2021, 30 (**8**): 080202. DOI: 10.1088/1674-1056/abeb08

Delta-Davidson method for interior eigenproblem in many-spin systems

Haoyu Guan(关浩宇) and Wenxian Zhang(张文献)
Chin. Phys. B, 2021, 30 (**3**): 030205. DOI: 10.1088/1674-1056/abd74a

A local refinement purely meshless scheme for time fractional nonlinear Schrödinger equation in irregular geometry region

Tao Jiang(蒋涛), Rong-Rong Jiang(蒋戎戎), Jin-Jing Huang(黄金晶), Jiu Ding(丁玖), and Jin-Lian Ren(任金莲)
Chin. Phys. B, 2021, 30 (**2**): 020202. DOI: 10.1088/1674-1056/abc0e0

Theoretical study of $(e,2e)$ triple differential cross section of $1b_{3g}$ orbital of ethylene by vibrational multi-center distorted-wave method

Zhenpeng Wang(王振鹏)[1], Maomao Gong(宫毛毛)[1,3,†], Xingyu Li(李星宇)[1], Songbin Zhang(张松斌)[3], and Xiangjun Chen(陈向军)[1,2,‡]

[1] *Hefei National Research Center for Physical Sciences at Microscale and Department of Modern Physics, University of Science and Technology of China, Hefei* 230026, *China*

[2] *Hefei National Laboratory, University of Science and Technology of China, Hefei* 230088, *China*

[3] *School of Physics and Information Technology, Shaanxi Normal University, Xi'an* 710119, *China*

(Received 18 June 2023; revised manuscript received 24 July 2023; accepted manuscript online 1 August 2023)

The vibrational motions are usually neglected when calculating (e,2e) triple differential cross sections (TDCSs) of molecules. Here, multi-center distorted-wave method (MCDW) has been modified by including molecular vibrations. This vibrational MCDW method is employed to calculate the TDCSs of $1b_{3g}$ orbital of ethylene at low (100 eV) and medium (250 eV) incident electron energies in coplanar asymmetric kinematic condition. The results show that molecular vibrations significantly influence the angular distributions of the TDCSs, especially in the binary region along momentum transfer near the Bethe ridge.

Keywords: (e,2e), multi-center distorted-wave method (MCDW), vibrational effect

PACS: 02.70.–c, 03.65.–w, 03.65.Nk **DOI:** 10.1088/1674-1056/acec45

1. Introduction

The electron-impact ionization is a fundamental process in atomic and molecular physics.[1] It plays an essential role in plasma physics, astrophysics, as well as in biological radiation physics. The accurate and reliable data of the ionization cross sections are of great importance both experimentally and theoretically. The complete information of the ionization dynamics can be obtained by the kinematically complete (e,2e) experiment, where the energies and momenta of the incoming and two outgoing electrons are determined. The quantity measured in such experiment is the so-called triple-differential cross sections (TDCSs). The experiments were usually performed at low (< 100 eV)[2,3] or medium (~ 250 eV)[4–7] incident energy employing traditional (e,2e) setup[8] or reaction microscope,[9] to test theoretical models concerning few-body dynamics in quantum mechanics.

For simple atoms and molecules,[10–13] the measured TDCSs can be reproduced by the nonperturbative theories such as the exterior complex scaling (ECS),[14] the converged close-coupling (CCC),[15] the time-dependent close-coupling (TDCC),[16] as well as the B-spline *R*-matrix[17] approaches. For more complex molecules, on the other hand, due to the multi-center character and the complex electronic structures, it is still challenging to precisely describe the electron-impact ionization cross sections. Perturbative methods are more practical. Madison *et al.* developed a molecular three-body distorted wave (M3DW) method[18–24] to calculate the TDCSs of molecules. In their approach, the continuum wave functions of the incident, scattered and ejected electrons are solved in a spherically averaged distorting potential. Due to the large computational quantities, the orientation-averaged molecular orbital (OAMO) approximation is usually adopted, which neglects the anisotropic property of the molecule. A proper average (PA) over orientation-dependent cross sections is also employed by the same authors[25–31] and the agreement between theory and experiment is generally improved. A multi-center distorted-wave (MCDW) method was reported by Zhang *et al.*[32] to describe the single-ionization dynamics for asymmetric kinematic conditions, and has been employed to calculate TDCSs for a series of molecules.[32–37] In the MCDW method, the incident and scattered electrons are described by plane waves, and the continuum wavefunction of the ejected electron is solved under the multi-center molecular ion potential. This method was recently extended to more general situations by including the distorted waves of the projectiles,[38,39] called multi-center three-distorted-wave (MCTDW) method. Mouawad *et al.*[40–43] investigated the TDCSs for molecules in the coplanar asymmetric geometry using a Coulomb wave and a simplified distorted wave methods within the first Born approximation.

Despite the great efforts of the theorists, discrepancies between experiments and theoretical calculations still remain. It is worth to note that, in all the theoretical methods concerning (e,2e) dynamics for molecular targets, the

†Corresponding author. E-mail: gongmm@ustc.edu.cn

‡Corresponding author. E-mail: xjun@ustc.edu.cn

© 2023 Chinese Physical Society and IOP Publishing Ltd

TDCSs were calculated at the equilibrium molecular geometry. However, according to some recent studies on electron momentum spectroscopy (EMS),[44–49] whose theoretical framework is the simple plane wave impulse approximation, molecular vibrational motions may have significant effect on the electron momentum distributions for molecular orbitals. Such effect has also been demonstrated in the temperature dependence of electronic transition probabilities,[50,51] electric dipole moment[52–54] and generalized oscillator strengths (GOSs)[55–60] of molecules. Therefore, it is highly necessary to develop a theoretical approach including vibrational motions for calculating (e,2e) TDCSs of molecules.

In the present work, the multi-center distorted-wave method[33] has been modified by including molecular vibrations. This vibrational multi-center distorted-wave method (v-MCDW) is then employed to calculate the (e,2e) TDCSs for the $1b_{3g}$ orbital of ethylene molecule. Typical kinematic arrangements in coplanar asymmetric geometry are chosen: 1) incident electron energy $E_i = 250$ eV with ejected electron energies $E_e = 8$ eV, 12 eV, 20 eV, 37 eV, 74 eV and scattering angles $\theta_s = -6°, -10°$; 2) incident electron energy $E_i = 100$ eV with ejected electron energies $E_e = 5$ eV, 10 eV, 15 eV and scattering angles $\theta_s = -6°, -10°$. A harmonic analytical quantum mechanical approach (HAQM)[44] is employed to include the vibrational motions of ethylene molecule in the calculations. The TDCSs calculated at equilibrium molecular geometry and including molecular vibrations are compared. The results show that the vibrational motions significantly influence the angular distributions of the TDCSs, especially in the binary region along momentum transfer near the Bethe ridge.

This paper is organized as follows: The theory of the v-MCDW[33] method is presented in Section 2. The calculated TDCSs including molecular vibrations and a comparison with the results calculated at equilibrium geometry are given in Section 3, followed by a summary in Section 4. Atomic units (a.u.) are used throughout the paper unless explicitly stated.

2. Theoretical method

2.1. Scattering theory of molecule under the Born–Oppenheimer approximation

According to the scattering theory, the electron impact single ionization process can be described by a transition matrix T_{fi} between the initial and final states of the scattering system through the interaction potential. Within the Born–Oppenheimer approximation and assuming that the rotational–vibrational coupling is small, the wave functions for the molecular target and ion can be written as a product of rotational, vibrational and electronic wave functions. Using the sum rule for the initial rotational states and closure relation for the final rotational states, the scattering amplitude can be written as

$$T_{fi}(\Omega) = \langle \Phi_f(\mathcal{R}_\Omega\{\boldsymbol{r}\})\chi_{fv'}(\boldsymbol{Q})| \times V(\{\boldsymbol{r}\})|\Phi_i(\mathcal{R}_\Omega\{\boldsymbol{r}\})\chi_{iv}(\boldsymbol{Q})\rangle, \quad (1)$$

where Φ_i and Φ_f are the initial and final electronic wavefunctions of the scattering system, respectively, depending on the nuclear coordinates $\boldsymbol{Q}$. $\mathcal{R}_\Omega$ is the rotation operator in the laboratory framework. $\Omega = (\alpha, \beta, \gamma)$ is the Euler angle which defines the molecular orientation. χ_{iv} and $\chi_{fv'}$ are the vibrational wave functions of the initial and final states. Summing over the final vibrational states, the magnitude squared of the transition matrix T_{fi} is

$$|T_{fi}(\Omega)|^2 = \sum_{v'} \langle \chi_{iv}(\boldsymbol{Q})|t_{fi}^*|\chi_{fv'}(\boldsymbol{Q})\rangle\langle\chi_{fv'}(\boldsymbol{Q})|t_{fi}|\chi_{iv}(\boldsymbol{Q})\rangle, \quad (2)$$

where the t_{fi} operator denotes the electronic transition. Using the closure relation for the final vibrational wavefunctions, Eq. (2) can be simplified as

$$|T_{fi}(\Omega,\boldsymbol{Q})|^2 = \int |\chi_{iv}(\boldsymbol{Q})|^2 |t_{fi}(\Omega,\boldsymbol{Q})|^2 \mathrm{d}\boldsymbol{Q}. \quad (3)$$

Due to the random distribution of molecular orientations in the experiment, the (e,2e) TDCS can be obtained by orientationally averaging the cross section

$$\frac{\mathrm{d}^3\sigma}{\mathrm{d}\Omega_e \mathrm{d}\Omega_s \mathrm{d}E_s} = \frac{1}{(2\pi)^5}\frac{k_e k_s}{k_i}\frac{1}{8\pi^2}\int |T_{fi}(\Omega,\boldsymbol{Q})|^2 \mathrm{d}\Omega, \quad (4)$$

where $\boldsymbol{k}_i$, $\boldsymbol{k}_s$ and $\boldsymbol{k}_e$ represent the momenta of the incident, scattered and ejected electrons, respectively. If we denote σ_e as the cross section scattering from the electronic wavefunction,

$$\sigma_e(\boldsymbol{Q}) = \frac{1}{(2\pi)^5}\frac{k_e k_s}{k_i}\frac{1}{8\pi^2}\int |t_{fi}(\Omega,\boldsymbol{Q})|^2 \mathrm{d}\Omega, \quad (5)$$

we have the TDCS for certain initial vibrational state v

$$\sigma_v = \frac{\mathrm{d}^3\sigma}{\mathrm{d}\Omega_e \mathrm{d}\Omega_s \mathrm{d}E_s} = \int |\chi_{iv}(\boldsymbol{Q})|^2 \sigma_e(\boldsymbol{Q})\mathrm{d}\boldsymbol{Q}. \quad (6)$$

Assuming a Boltzmann distribution $P_v(T)$ at temperature T for initial vibrational states, the (e,2e) TDCS for a molecular target considering vibrational motions will be

$$\sigma_{ave} = \sum_v P_v(T)\int |\chi_{iv}(\boldsymbol{Q})|^2 \sigma_e(\boldsymbol{Q})\mathrm{d}\boldsymbol{Q}. \quad (7)$$

2.2. Multi-center distorted wave method

In the present coplanar asymmetric kinematic arrangements, the incident and scattered electrons are moving fast, and can be approximately described by the plane waves. In the MCDW method, the electronic scattering amplitude $t_{fi}(\Omega)$ can be expressed as[33]

$$t_{fi}(\Omega) = \langle \psi_f(\boldsymbol{k}_e; \mathcal{R}_\Omega(\{\boldsymbol{r}\}))\boldsymbol{k}_s|V(\{\boldsymbol{r}\})|\psi_i(\mathcal{R}_\Omega(\{\boldsymbol{r}\}))\boldsymbol{k}_i\rangle, \quad (8)$$

where V denotes the interaction between the incident electron and the molecule, which can be written as

$$V = \sum_j^N \frac{1}{|\boldsymbol{r}_j - \boldsymbol{r}_i|} - \sum_n \frac{Z_n}{|\boldsymbol{R}_n - \boldsymbol{r}_i|}. \quad (9)$$

where $\boldsymbol{r}_{\rm i}$ and $\boldsymbol{r}_j$ are the position vectors for the incoming electron and the jth bound electron of the target, respectively. Under the sudden approximation, $t_{\rm fi}$ can be simplified as

$$t_{\rm fi}(\Omega) = \frac{4\pi}{K^2}\langle \mathcal{F}^{(-)}(\boldsymbol{k}_{\rm e};\mathcal{R}_\Omega \boldsymbol{r})|\,{\rm e}^{{\rm i}\boldsymbol{K}\cdot\boldsymbol{r}} - \frac{\sum_n Z_n\,{\rm e}^{{\rm i}\boldsymbol{K}\cdot\boldsymbol{R}_n}}{N}|\phi_\alpha(\mathcal{R}_\Omega \boldsymbol{r})\rangle, \tag{10}$$

where the Bethe integral technique is used. $\boldsymbol{K} = \boldsymbol{k}_{\rm i} - \boldsymbol{k}_{\rm s}$ denotes the momentum transfer. ϕ_α is the wave function of the ionized bound orbital. $\mathcal{F}^{(-)}$ is the continuum wave function of the ejected electron, which is solved under the multi-center molecular ion potential:

$$\left(-\frac{1}{2}\nabla^2 + V^{\rm m} - E_{\rm e}\right)\mathcal{F}^{(-)}(\boldsymbol{k}_{\rm e},\boldsymbol{r}) = 0, \tag{11}$$

where $V^{\rm m} = V^{\rm st} + V^{\rm cp}$ is the model potential.[61] $V^{\rm st}$ and $V^{\rm cp}$ are the static and correlation-polarization potentials, respectively. The single-center expansion is used to solve the equation, in which the wave function and potential are expanded by the symmetry-adapted angular functions.[61–63] Substituting Eq. (10) into Eq. (5), $\sigma_{\rm e}$ is then obtained by averaging over all possible molecular orientations.

2.3. Harmonic analytical quantum mechanical approach

In order to take into account the molecular vibrations, HAQM approach[44] is adopted. In this approach, the vibrational wave function χ_{iv} is approximated by the product of the harmonic oscillator functions ξ_{vL}. Then Eq. (6) can be written as

$$\sigma_v = \int \prod_L |\xi_{vL}(\boldsymbol{Q}_L)|^2 \sigma_{\rm e}(\boldsymbol{Q})\,{\rm d}\boldsymbol{Q}, \tag{12}$$

where Q_L is the displacement from the equilibrium geometry along the normal coordinate of the Lth mode. $\sigma_{\rm e}$ can be expanded in terms of the normal coordinates around the equilibrium geometry ($\boldsymbol{Q}_0$)

$$\sigma_{\rm e}(\boldsymbol{Q}) \approx \sigma_{\rm e}(\boldsymbol{Q}_0) + \sum_L Q_L \frac{\partial \sigma_{\rm e}(\boldsymbol{Q})}{\partial Q_L}\bigg|_{\boldsymbol{Q}=\boldsymbol{Q}_0} + \frac{1}{2!}\left(\sum_L Q_L \frac{\partial}{\partial Q_L}\right)^2 \sigma_{\rm e}(\boldsymbol{Q})\bigg|_{\boldsymbol{Q}=\boldsymbol{Q}_0} + \frac{1}{3!}\left(\sum_L Q_L \frac{\partial}{\partial Q_L}\right)^3 \sigma_{\rm e}(\boldsymbol{Q})\bigg|_{\boldsymbol{Q}=\boldsymbol{Q}_0} + \cdots. \tag{13}$$

Substituting Eq. (13) into Eq. (12), we can get

$$\sigma_v(\boldsymbol{Q}) = \sigma_{\rm e}(\boldsymbol{Q}_0) + \frac{1}{2!}\sum_L \frac{\partial^2 \sigma_{\rm e}}{\partial Q_L^2}\bigg|_{\boldsymbol{Q}=\boldsymbol{Q}_0}\langle \xi_{vL}|Q_L^2|\xi_{vL}\rangle + \frac{1}{4!}\sum_L \frac{\partial^4 \sigma_{\rm e}}{\partial Q_L^4}\bigg|_{\boldsymbol{Q}=\boldsymbol{Q}_0}\langle \xi_{vL}|Q_L^4|\xi_{vL}\rangle + \left(\frac{1}{2!}\right)^2 \sum_{L\neq M} \frac{\partial^4 \sigma_{\rm e}}{\partial Q_L^2 \partial Q_M^2}\bigg|_{\boldsymbol{Q}=\boldsymbol{Q}_0} \times \langle \xi_{vL}|Q_L^2|\xi_{vL}\rangle\langle \xi_{vL}|Q_M^2|\xi_{vL}\rangle + \cdots. \tag{14}$$

Here, the property of the harmonic oscillator function of $\langle \xi_{vL}|Q_L^{2n+1}|\xi_{vL}\rangle = 0$ is used. Assume that $\sigma_v(\boldsymbol{Q})$ changes slowly with $\boldsymbol{Q}$ around the equilibrium geometry so that the higher-order terms in Eq. (14) can be neglected.[44] Equation (12) can then be expressed as

$$\sigma_v(\boldsymbol{Q}) = \sigma_{\rm e}(\boldsymbol{Q}_0) + \sum_L \left(\frac{1}{2!}\frac{\partial^2 \sigma_{\rm e}}{\partial Q_L^2}\bigg|_{\boldsymbol{Q}=\boldsymbol{Q}_0}\langle \xi_{vL}|Q_L^2|\xi_{vL}\rangle + \frac{1}{4!}\frac{\partial^4 \sigma_{\rm e}}{\partial Q_L^4}\bigg|_{\boldsymbol{Q}=\boldsymbol{Q}_0}\langle \xi_{vL}|Q_L^4|\xi_{vL}\rangle + \cdots\right). \tag{15}$$

Equation (15) can further be written as a sum of the contributions of each vibrational normal mode

$$\sigma_v(\boldsymbol{Q}) = \sigma_{\rm e}(\boldsymbol{Q}_0) + \sum_L \langle \xi_{vL}|\sigma_{\rm e}(Q_L\widehat{q}_L) - \sigma_{\rm e}(\boldsymbol{Q}_0)|\xi_{vL}\rangle, \tag{16}$$

where $\widehat{q}_L$ is the unit vector along the Lth normal coordinate. Equation (16) is the basic equation of the v-MCDW approach, the first term of which is the TDCS at the equilibrium geometry and the second term represents the vibrational effects.

In the practical calculation, we assume that the vibrational contributions of each vibrational mode can be approximately written as quadratic polynomials of the normal coordinates. Assuming a Boltzmann distribution for the initial vibrational states, the vibrationally averaged TDCS can finally be written as

$$\sigma_{\rm ave} = \sigma_{\rm e}(\boldsymbol{Q}_0) + \Sigma_{nL} P_{nL}(T)\left[\frac{\hbar}{2\omega_L}(2n_L+1)c_{L,2} + 3\left(\frac{\hbar}{2\omega_L}\right)^2 (2n_L^2 + 2n_L + 1)c_{L,4}\right], \tag{17}$$

where $P_{nL}(T)$ represents the probability in the vibrational level v and vibrational mode L at temperature T, n_L and ω_L are the vibrational quantum number and angular frequency of the Lth normal mode, respectively. $c_{L,2}$ and $c_{L,4}$ represent the quadratic polynomials fitting coefficients. In order to obtain $c_{L,2}$ and $c_{L,4}$, a set of $\sigma_{\rm e}$ are calculated at equilibrium and distorted geometries, which satisfy

$$|\xi_{vL}(\boldsymbol{Q}_0 + Q_L)|^2 / |\xi_{vL}(\boldsymbol{Q}_0)|^2 = 1,\ 3/4,\ 1/2,\ 1/4,\ 1/8,\ 1/16. \tag{18}$$

Equilibrium geometry ($\boldsymbol{Q}_0$) is optimized at MP2[64–68]/aug-cc-pVTZ[69] level using Gaussian 09.[70] The vibrational normal coordinates and vibrational frequency for the electronic ground state are calculated at MP2/aug-cc-pVTZ level and the wave functions of bound orbitals are obtained with B3LYP[71,72]/aug-cc-pVTZ using Gaussian 09 program. The frequencies of all the vibrational modes are listed in Table 1, in good agreement with the experimental data.[73] In the calculation of TDCSs, the upper limits of partial wave expansions for

the bound and the continuum wave functions are $l_{\rm bmax} = 16$ and $l_{\rm cmax} = 28$, respectively. The Euler angle meshes for the orientation spherical average are $N_\alpha = 20$, $N_\beta = 16$, $N_\gamma = 20$, where N_α, N_β and N_γ are the point numbers of numerical integrals for Euler angle α, β and γ. In the single-center expansion, r_j ranges from 0 to 8.47 a.u. with increasing step size from 0.001 a.u. to 0.128 a.u.

Table 1. Vibrational frequency of ethylene.

Mode	Vibrational description	Calculated (cm^{-1})	Experiment[73] (cm^{-1})
ν_1	CH_2 sym. stretch (A_g)	3192	3022
ν_2	C = C stretch (A_g)	1678	1625
ν_3	CH_2 sym. scissors (A_g)	1380	1344
ν_4	torsion (A_u)	1047	1026
ν_5	CH_2 asym. stretch (B_{3g})	3261	3083
ν_6	CH_2 rock (B_{3g})	1245	1222
ν_7	CH_2 wag (B_{3u})	976	949
ν_8	CH_2 wag (B_{2g})	946	940
ν_9	CH_2 asym. stretch (B_{2u})	3288	3105
ν_{10}	CH_2 rock (B_{2u})	823	826
ν_{11}	CH_2 sym. stretch (B_{2u})	3172	2989
ν_{12}	CH_2 scissors (B_{1u})	1479	1444

3. Results and discussion

At equilibrium geometry, ethylene molecule belongs to D_{2h} point group and its ground-state electronic configuration[74] is $(\text{core})^4(2a_g)^2(2b_{1u})^2(1b_{2u})^2(3a_g)^2(1b_{3g})^2(1b_{3u})^2$. In the present work, the (e,2e) TDCSs of $1b_{3g}$ orbital of ethylene are calculated by the MCDW method. Figure 1 shows the calculated three-dimensional (3D) angular distributions of the TDCSs for $1b_{3g}$ orbital as a function of outgoing direction of the ejected electron at $E_i = 250$ eV, $E_e = 8$ eV and $\theta_s = -10°$. Figure 1(a) is the result calculated by the normal MCDW method at equilibrium geometry, and Fig. 1(b) is that calculated by the v-MCDW method. In these 3D images, the magnitude of the TDCS for a given direction of ejected electron is expressed by the distance from the origin to the point on the surface. The incident electron ($\boldsymbol{k}_i$) moves along the z axis and is scattered with a momentum $\boldsymbol{k}_s$ and a scattering angle θ_s. $\boldsymbol{k}_i$, $\boldsymbol{k}_s$ as well as the momentum transfer vector $\boldsymbol{K}$ lie in the xz plane, i.e., the scattering plane. The binary peak along the direction of momentum transfer results from the binary collision between the incident and orbital electrons, while the recoil peak in opposite direction is regarded as the backward reflection from the residual ion of the ejected electron. Under this kinematic condition, $|\boldsymbol{K}| = 0.754$ a.u. and $|\boldsymbol{k}_e| = 0.767$ a.u., which is near the Bethe ridge, the incident electron transfers almost all the changed momentum to the active bound electron. At this near the Bethe ridge kinematics, the shape of the binary peak reflects the electron momentum profile of the ionized molecular orbital. In Fig. 1(a), there is an obvious dip in the direction of the momentum transfer, indicating a p-type character of the $1b_{3g}$ orbital, while the intensity of the TDCS has obviously been enhanced along the momentum transfer after considering the vibrational effect, indicating that the molecular nuclear motions significantly affect the (e,2e) TDCSs.

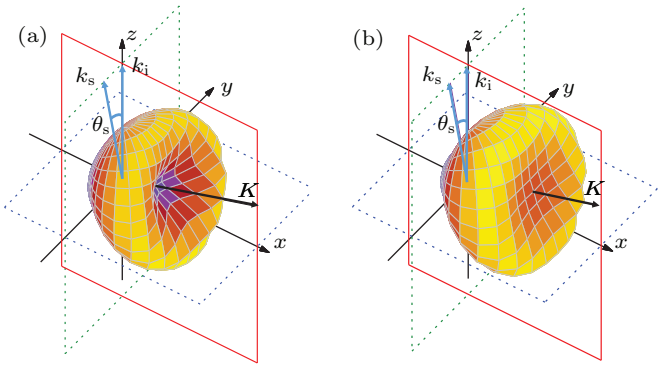


Fig. 1. Three-dimensional angular distributions of TDCSs for $1b_{3g}$ orbital of ethylene molecule at $E_i = 250$ eV, $E_e = 8$ eV and $\theta_s = -10°$ calculated by (a) MCDW method at equilibrium geometry, (b) vibrational MCDW method.

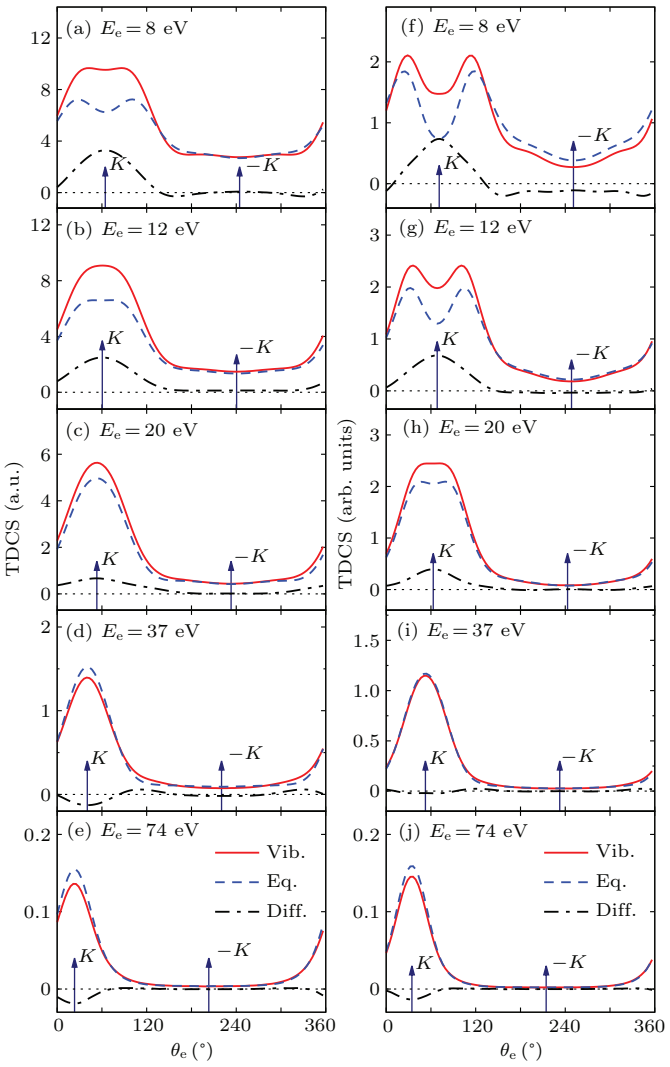


Fig. 2. The TDCSs for electron impact (250 eV) single ionization of $1b_{3g}$ orbital of ethylene molecule in the coplanar asymmetric geometry. The ejected electron energy is displayed in each figure. Left column: $\theta_s = -6°$; right column: $\theta_s = -10°$.

In order to explore in detail the vibrational effect on TDCS, two typical kinematic arrangements in coplanar asym-

metric geometry are investigated: 1) incident electron energy $E_i = 250$ eV with ejected electron energies $E_e = 8$ eV, 12 eV, 20 eV, 37 eV, 74 eV and scattering angles $\theta_s = -6°$, $-10°$; 2) incident electron energy $E_i = 100$ eV with ejected electron energies $E_e = 5$ eV, 10 eV, 15 eV and scattering angles $\theta_s = -6°$, $-10°$. The results are plotted in Figs. 2 and 3, respectively. The left column of Fig. 2 shows the TDCSs in the scattering plane for (a) $E_e = 8$ eV, (b) $E_e = 12$ eV, (c) $E_e = 20$ eV, (d) $E_e = 37$ eV and (e) $E_e = 74$ eV with scattering angle fixed at $\theta_s = -6°$. The dashed blue lines represent the TDCSs calculated by the normal MCDW at equilibrium geometry, while the solid red lines represent the results calculated by the v-MCDW including molecular vibrations. The dot dashed black lines are their difference that can be regarded as the total contributions from all the vibrational modes. In Figs. 2(a)–2(c), the molecular vibrations enhance the binary peaks relative to the equilibrium geometry, while for higher ejected electron energies in Figs. 2(d) and 2(e), a weak negative influence can be observed. The similar behavior is also observed for scattering angle $\theta_s = -10°$ as shown in the right column of Fig. 2. For low ejected electron energies ($E_e = 8$ eV, 12 eV), the binary peak exhibits a double-peak structure with a dip near the direction of momentum transfer. This double-peak structure tends to merge into a single peak as the ejected electron energy increases. The binary region is strongly influenced by molecular vibrations both in shape and intensity for lower ejected electron energy and this double-peak structure becomes flattened when including vibrational motions. The recoil peaks in Fig. 2, on the other hand, are not sensitive to the molecular vibrations.

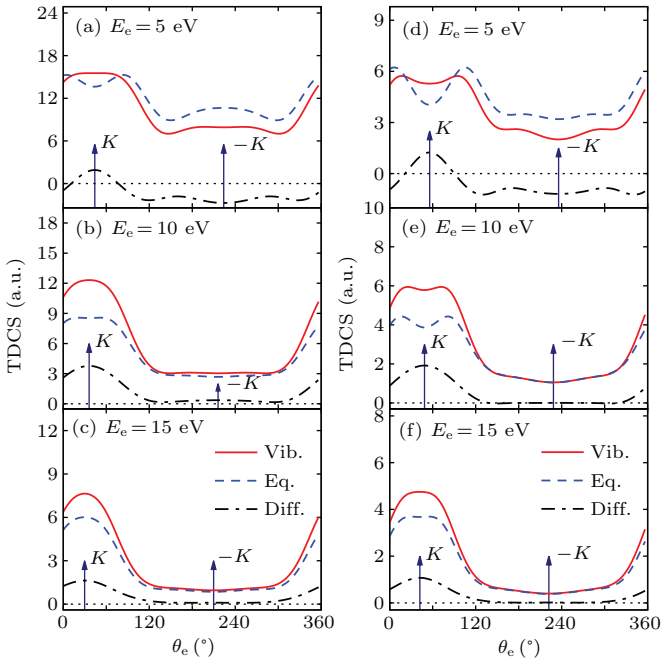


Fig. 3. The TDCSs for electron impact (100 eV) single ionization of $1b_{3g}$ orbital of ethylene molecule in the coplanar asymmetric geometry. The ejected electron energy is displayed in each figure. Left column: $\theta_s = -6°$; right column: $\theta_s = -10°$.

As we have mentioned, for $E_i = 250$ eV, $E_e = 8$ eV and $\theta_s = -10°$, which is near the Bethe ridge, the incident electron transfers almost all the changed momentum to the target electron to ensure a clean knock out. The shape of the binary peak reflects the electron momentum profile of $1b_{3g}$ orbital of ethylene molecule as shown in Fig. 2(f), through the relation between the ejection angle θ_e and the magnitude of orbital electron momentum p, which can be easily obtained through the energy and momentum conservations in the ionization process. The relationship between p and θ_e can be expressed as

$$p(\theta_e) = \sqrt{(k_e \cos\theta_e + k_s \cos\theta_s - k_i)^2 + (k_e \sin\theta_e + k_s \sin\theta_s)^2}. \tag{19}$$

At Bethe ridge condition, p will approach to 0 if the ionized electron is ejected along the direction of momentum transfer vector $\boldsymbol{K}$, corresponding to the center of the binary peak. In other words, the TDCS distribution near the direction of $\boldsymbol{K}$ characterizes the low momentum area in the electron momentum profile of molecular orbital. From the EMS study of Watanabe *et al.*,[44] the $1b_{3g}$ orbital of ethylene has a p-type momentum profile, having zero intensity at zero momentum (regardless of experimental momentum resolution). This leads to the deep dip in the middle of the binary peak in Figs. 2(a), 2(f) and 2(g). With the increase of the ejected electron energy, the kinematic condition gradually deviates from the Bethe ridge and p will also deviate from zero at the direction of $\boldsymbol{K}$, therefore the double binary peak merges into a single one from Fig. 2(a) to Fig. 2(e) and Fig. 2(f) to Fig. (j).

Figure 4 shows the contributions of individual vibrational modes on TDCS at $E_i = 250$ eV, $E_e = 8$ eV and $\theta_s = -10°$ with the pictorial representations of each vibrational modes shown in the lower panel. All the twelve vibrational modes of ethylene are included in the calculations. They belong to four types of point group symmetries: D_{2h} (ν_1, ν_2 and ν_3), D_2 (ν_4), C_{2h} (ν_5, ν_6 and ν_8), and C_{2v} (ν_7, ν_9, ν_{10}, ν_{11} and ν_{12}). It is shown in the figure that the CH_2 asymmetric stretch (ν_5), CH_2 rock (ν_6), and CH_2 wag (ν_8), which belong to C_{2h} point group, have the most significant influence on the TDCS. All the vibrational modes lead to the enhanced intensity at $\boldsymbol{K}$, resulting in the flattening of the double-peak structure for the binary peak.

Figure 3 shows the TDCSs at incident electron energy $E_i = 100$ eV with $E_e = 5$ eV, 10 eV and 15 eV and scattered angle $\theta_s = -6°$, $-10°$. The similar behavior is observed in the binary region as in the case of $E_i = 250$ eV. For lowest ejected electron energies ($E_e = 5$ eV), the binary peak exhibits a double-peak structure with a dip near the momentum transfer direction. This double-peak structure tends to merge into a single peak as the ejected electron energy increases. The binary peaks are also significantly influenced by the molecular vibrations both in shape and intensity, not only enhanced but

also flattened at higher ejected electron energies. As for the recoil region, the TDCSs are significantly reduced at $E_e = 5$ eV when considering vibrational motions, while the vibrational effect can be neglected for higher ejected electron energies.

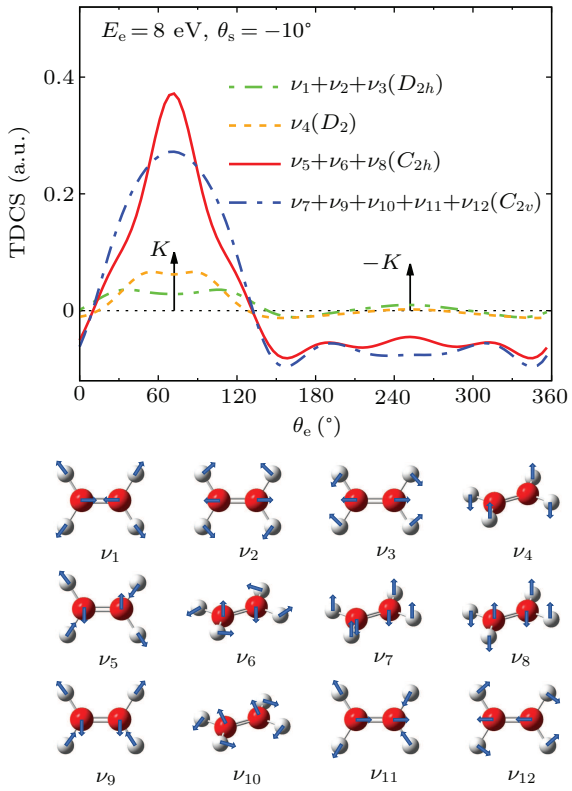


Fig. 4. Contributions of all vibrational modes, which are divided by symmetry, on the TDCSs distributions of $1b_{3g}$ orbital of ethylene molecule at $E_e = 8$ eV and $\theta_s = -10°$. The lower panel shows the pictorial representations of vibrational modes.

4. Summary

In summary, we have calculated the TDCSs for electron-impact single ionization from the $1b_{3g}$ orbital of ethylene molecule in the coplanar asymmetric geometry at the incident electron energies of 250 eV and 100 eV using the MCDW method modified by including molecular vibrations. The results show that molecular vibrations have significant influence on the angular distributions of the TDCSs both in shape and in intensity, especially in the binary region near the Bethe ridge. The binary peak exhibits a double-peak structure with a dip along the direction of momentum transfer, which is directly related to the p-type electron momentum profile of $1b_{3g}$ orbital. This double-peak structure becomes flattened when including vibrational motions in the calculation. The analysis of the contributions of individual vibrational modes shows that the CH_2 asymmetric stretch (ν_5), CH_2 rock (ν_6), and CH_2 wag (ν_8), which belong to C_{2h} point group, have the most significant influence on the TDCSs. The present study indicates that molecular vibration needs to be considered when we want to precisely describe the electron-impact ionization dynamics of molecules. It also suggests that molecular vibration may affect a wide range of molecular processes induced by ion collisions and photo-absorption, not only influence cross sections but may also change the dipole-forbidden transitions.

Acknowledgements

Project supported by the National Natural Science Foundation of China (Grant Nos. 12004370 and 12127804) and the Strategic Priority Research Program of the Chinese Academy of Sciences (Grant No. XDB34020000).

References

[1] Taylor J R 1972 *Scattering theory: quantum theory of nonrelativistic collisions* (Wiley)
[2] Hossen K, Ren X, Wang E, Gong M, Li X, Zhang S B, Chen X and Dorn A 2018 *J. Phys. B: At. Mol. Opt. Phys.* **51** 215201
[3] Wang E, Ren X, Gong M, Ali E, Wang Z, Ma C, Madison D, Chen X and Dorn A 2020 *Phys. Rev. A* **102** 062813
[4] Jones D B, Ali E, Ning C G, Ferreira da Silva F, Ingólfsson O, Lopes M C A, Chakraborty H S, Madison D H and Brunger M J 2019 *J. Chem. Phys.* **151** 124306
[5] Jones D B, Ali E, Ning C G, Colgan J, Ingólfsson O, Madison D H and Brunger M J 2016 *J. Chem. Phys.* **145** 164306
[6] Colyer C J, Stevenson M A, Al-Hagan O, Madison D H, Ning C G and Lohmann B 2009 *J. Phys. B: At. Mol. Opt. Phys.* **42** 235207
[7] Milne-Brownlie D S, Cavanagh S J, Lohmann B, Champion C, Hervieux P A and Hanssen J 2004 *Phys. Rev. A* **69** 032701
[8] Cavanagh S J and Lohmann B 1999 *J. Phys. B: At. Mol. Opt. Phys.* **32** L261
[9] Ullrich J, Moshammer R, Dorn A, Döorner R, Schmidt L P H and Schmidt-Böocking H 2003 *Rep. Prog. Phys.* **66** 1463
[10] Kheifets A S 2005 *Phys. Rev. A* **71** 022704
[11] Kheifets A S and Bray I 2005 *Phys. Rev. A* **72** 022703
[12] Vanroose W, Horner D A, Martín F, Rescigno T N and McCurdy C W 2006 *Phys. Rev. A* **74** 052702
[13] Colgan J, Pindzola M S, Robicheaux F, Kaiser C, Murray A J and Madison D H 2008 *Phys. Rev. Lett.* **101** 233201
[14] Rescigno T N, Baertschy M, Isaacs W A and McCurdy C W 1999 *Science* **286** 2474
[15] Dorn A, Kheifets A, Schröter C D, Najjari B, Höhr C, Moshammer R and Ullrich J 2001 *Phys. Rev. Lett.* **86** 3755
[16] Pindzola M S and Schultz D R 1996 *Phys. Rev. A* **53** 1525
[17] Zatsarinny O and Bartschat K 2011 *Phys. Rev. Lett.* **107** 2011
[18] Gao J, Madison D H and Peacher J L 2005 *Phys. Rev. A* **72** 032721
[19] Gao J, Peacher J L and Madison D H 2005 *J. Chem. Phys.* **123** 204302
[20] Gao J, Madison D H and Peacher J L 2005 *J. Chem. Phys.* **123** 204314
[21] Gao J, Madison D H and Peacher J L 2005 *Phys. Rev. A* **72** 020701
[22] Gao J, Madison D H, Peacher J L, Murray A J and Hussey M J 2006 *J. Chem. Phys.* **124** 194306
[23] Gao J, Madison D H and Peacher J L 2006 *J. Phys. B: At. Mol. Opt. Phys.* **39** 1275
[24] Madison D and Al-Hagan O 2010 *J. At. Mol. Opt. Phys.*
[25] Chaluvadi H, Ning C G and Madison D 2014 *Phys. Rev. A* **89** 062712
[26] Ali E, Nixon K, Murray A, Ning C, Colgan J and Madison D 2015 *Phys. Rev. A* **92** 042711
[27] Jones D B, Ali E, Nixon K L, Limao-Vieira P, Hubin-Franskin M J, Delwiche J, Ning C G, Colgan J, Murray A J, Madison D H, *et al.* 2015 *J. Chem. Phys.* **143** 184310
[28] Ren X, Amami S, Hossen K, Ali E, Ning C, Colgan J, Madison D and Dorn A 2017 *Phys. Rev. A* **95** 022701
[29] Jones D B, Ali E, Ning C G, Ferreira da Silva F, Ingólfsson O, Lopes M C A, Chakraborty H S, Madison D H and Brunger M J 2019 *J. Chem. Phys.* **151** 124306
[30] Ali E, Chakraborty H S and Madison D H 2020 *J. Chem. Phys.* **152** 124303
[31] Jones D, Ali E, Chakraborty H, Ning C, García G, Madison D and Brunger M 2021 *Chem. Phys. Lett.* **781** 139000
[32] Zhang S b, Li X Y, Wang J G, Qu Y Z and Chen X 2014 *Phys. Rev. A* **89** 052711

[33] Li X, Gong M, Liu L, Wu Y, Wang J, Qu Y and Chen X 2017 *Phys. Rev. A* **95** 012703
[34] Gong M, Li X, Zhang S B, Liu L, Wu Y, Wang J, Qu Y and Chen X 2017 *Phys. Rev. A* **96** 042703
[35] Xu X, Gong M, Li X, Zhang S B and Chen X 2018 *J. Chem. Phys.* **148** 244104
[36] Wang Z, Gong M, Li X, Zhang S B and Chen X 2021 *J. Electron Spectrosc. Relat. Phenom.* **248** 147059
[37] Wang Y, Wang Z, Gong M, Xu C and Chen X 2022 *Chin. Phys. B* **31** 010202
[38] Gong M, Li X, Zhang S B, Niu S, Ren X, Wang E, Dorn A and Chen X 2018 *Phys. Rev. A* **98** 042710
[39] Gong M, Wang Z, Li X, Zhang S B and Chen X 2020 *J. Phys. B: At. Mol. Opt. Phys.* **54** 015206
[40] Mouawad L, Hervieux P A, Cappello C D, Pansanel J, Osman A, Khalil M and Bitar Z E 2017 *J. Phys. B: At. Mol. Opt. Phys.* **50** 215204
[41] Mouawad L, Hervieux P A, Cappello C D, Pansanel J, Robert V and Bitar Z E 2018 *J. Phys. B: At. Mol. Opt. Phys.* **51** 175201
[42] Mouawad L, Hervieux P A, Cappello C D, Pansanel J, Robert V and Bitar Z E 2019 *Eur. Phys. J. D* **73** 76
[43] Mouawad L, Hervieux P A, Cappello C D and Bitar Z E 2019 *J. Phys. B: At. Mol. Opt. Phys.* **53** 025202
[44] Watanabe N, Yamazaki M and Takahashi M 2012 *J. Chem. Phys.* **137** 114301
[45] Watanabe N, Yamazaki M and Takahashi M 2014 *J. Chem. Phys.* **141** 244314
[46] Morini F, Deleuze M S, Watanabe N and Takahashi M 2015 *J. Chem. Phys.* **142** 094308
[47] Tang Y, Shan X, Yang J, Niu S, Zhang Z, Watanabe N, Yamazaki M, Takahashi M and Chen X 2016 *J. Phys. Chem. A* **120** 6855
[48] Tang Y, Shan X, Niu S, Liu Z, Wang E, Watanabe N, Yamazaki M, Takahashi M and Chen X 2017 *J. Phys. Chem. A* **121** 277
[49] Liu Z, Tang Y, Niu S, Shan X, Xu C and Chen X 2020 *J. Phys. Chem. A* **124** 8551
[50] Saito K, Eishiro Y, Nakao Y, Sato H and Sakaki S 2012 *Inorg. Chem.* **51** 2785
[51] Inkinen J, Niskanen J, Sakko A, Ruotsalainen K O, Pylkkänen T, Galambosi S, Hakala M, Monaco G, Hämäläinen K and Huotari S 2014 *J. Phys. Chem. A* **118** 3288
[52] Puzzarini C and Taylor P R 2005 *J. Chem. Phys.* **122** 054315
[53] Arapiraca A F C, Jonsson D and Mohallem J R 2011 *J. Chem. Phys.* **135** 244313
[54] Arapiraca A and Mohallem J 2014 *Chem. Phys. Lett.* **609** 123
[55] Watanabe N, Suzuki D and Takahashi M 2011 *J. Chem. Phys.* **134** 234309
[56] Watanabe N, Hirayama T, Suzuki D and Takahashi M 2013 *J. Chem. Phys.* **138** 184311
[57] Watanabe N and Takahashi M 2014 *J. Phys. B: At. Mol. Opt. Phys.* **47** 155203
[58] Watanabe N, Hirayama T and Takahashi M 2019 *Phys. Rev. A* **99** 062708
[59] Watanabe N and Takahashi M 2020 *J. Phys. B: At. Mol. Opt. Phys.* **53** 075202
[60] Watanabe N and Takahashi M 2021 *J. Phys. B: At. Mol. Opt. Phys.* **54** 135202
[61] Sanna N and Gianturco F 2000 *Comput. Phys. Commun.* **128** 139
[62] Sanna N and Morelli G 2004 *Comput. Phys. Commun.* **162** 51
[63] Sanna N, Baccarelli I and Morelli G 2009 *Comput. Phys. Commun.* **180** 2544
[64] Head-Gordon M, Pople J A and Frisch M J 1988 *Chem. Phys. Lett.* **153** 503
[65] Sæbø S and Almlöf J 1989 *Chem. Phys. Lett.* **154** 83
[66] Frisch M J, Head-Gordon M and Pople J A 1990 *Chem. Phys. Lett.* **166** 275
[67] Frisch M J, Head-Gordon M and Pople J A 1990 *Chem. Phys. Lett.* **166** 281
[68] Head-Gordon M and Head-Gordon T 1994 *Chem. Phys. Lett.* **220** 122
[69] Dunning T H 1989 *J. Chem. Phys.* **90** 1007
[70] Frisch M J, Trucks G W, Schlegel H B, Scuseria G E, Robb M A, Cheeseman J R, Scalmani G, Barone V, Petersson G A, Nakatsuji H, *et al*. 2009 Gaussian 09, Revision A.02, Technical Report
[71] Becke A D 1993 *J. Chem. Phys.* **98** 5648
[72] Lee C, Yang W and Parr R G 1988 *Phys. Rev. B* **37** 785
[73] Sension R J and Hudson B S 1989 *J. Chem. Phys.* **90** 1377
[74] Hollebone B, Neville J, Zheng Y, Brion C, Wang Y and Davidson E 1995 *Chem. Phys.* **196** 13